Jurnal Kejuruteraan 35(4) 2023: 823-830
https://doi.org/10.17576/jkukm-2023-35(4)-04

Pterygium Classification Using Deep Patch Region-based Anterior Segment Photographed Images

Nurul Syahira Mohamad Zamani[a], W Mimi Diyana W Zaki[a*], Aqilah Baseri Huddin[a], Haliza Abdul Mutalib[b] & Aini Hussain[a]

[a]*Department of Electrical, Electronic and Systems Engineering, Faculty of Engineering and Built Environment, Universiti Kebangsaan Malaysia, 43600 UKM Bangi, Malaysia*
[b]*Optometry and Vision Sciences Programme, Faculty of Health Sciences, School of Healthcare Sciences, Universiti Kebangsaan Malaysia, 50300 Kuala Lumpur, Malaysia*

**Corresponding author: wmdiyana@ukm.edu.my*

Received 14 October 2022, Received in revised form 9 December 2022
Accepted 10 January 2023, Available online 30 July 2023

ABSTRACT

Early pterygium screening is crucial to avoid blurred vision caused by cornea and pupil encroachment. However, medical assessment and conventional screening could be laborious and time-consuming to be implemented. This constraint seeks an advanced yet efficient automated pterygium screening to assist the current diagnostic method. Patch region-based anterior segment photographed images (ASPIs) focus the feature on a particular region of the pterygium growth. This work addresses the data limitation on deep neural network (DNN) processing with large-scale data requirements. It presents an automated pterygium classification of patch region-based ASPI using our previous re-establish network, "VggNet16-wbn", the VggNet16, with the addition of batch normalisation layer after each convolutional layer. During an image pre-processing step, the pterygium and nonpterygium tissue are extracted from ASPI, followed by the generation of a single and three-by-three image patch region-based on the size of the 85×85 dataset. Data preparation with 10-fold cross-validation has been conducted to ensure the data are well generalised to minimise the probability of underfitting and overfitting problems. The proposed experimental work has successfully classified the pterygium tissue with more than 99% accuracy, sensitivity, specificity, and precision using appropriate hyperparameters values. This work could be used as a baseline framework for pterygium classification using limited data processing.

Keywords: Anterior segment photographed image (ASPI); Automated pterygium screening; Patch region-based; Deep neural network (DNN); Pterygium classification

INTRODUCTION

An anterior eye disease involves anterior parts of the eye, such as the cornea, which are frequently exposed to ultraviolet (UV) radiation (UVR). Ophthalmoheliosis is a class of eye disease that associates eye conditions with UVR aetiology (Bogdănici et al. 2013; M. T. Coroneo et al. 1991). The emitted UV light contains radiations which can lead to light damage to the exposed eye. The eyes are tremendously sensitive to light compared to the skin. UVR in sunlight could affect the lens and retina when high wavelengths penetrate the cornea (Yam & Kwok 2014). The cornea is located at the eye's outermost layer and receives the most UVR exposure. This condition causes a chronic effect and significantly impacts eye diseases such as cataracts, pterygium and droplet keratopathy (Vanicek et al. 2000).

The abnormal tissue formation, such as fibrovascular tissue on the conjunctiva, is related to excessive UVR exposure (Asokan et al. 2012; M. Coroneo 2011; Lucas et al. 2008; Paula et al. 2006). This abnormal tissue appears in a yellowish spot called pinguecula (Asokan et al. 2012; Le et al. 2015). Pinguecula anterior eye disease tends to grow faster and encroach into the corneal area with UVR exposure. This fibrovascular tissue encroachment has known as pterygium anterior eye disease (Abdani et al. 2015; Kwok & Coroneo 1994; Panchapakesan et al. 1998). Besides the UVR exposure, the dry eye condition and the presence of wind and dust can also be factored in the presence of abnormal tissue (Zamani et al. 2020). The pterygium growth is usually triangular- and winged-shaped near the nasal area of the left and right eye (Anbesse et al. 2017; Hill 1989; Kwok & Coroneo 1994; Panchapakesan et al. 1998; Twelker et al. 2000). Fortunately, pinguecula and pterygium tissues cause no harm to the patients as they are categorized as noncancerous abnormal tissue (Taylor 1989; Viso et al. 2011). However, if the tissue proliferates, it is likely to cause visual impairment resulting in vision loss. Hence, precautions must be taken to avoid this consequence, such as wearing sunglasses during outdoor activities and avoiding UV exposure for a long period.

The appearance of pterygium tissue can be seen and validated by the expert, an ophthalmologist, through earlier

screening using slit lamp examination (Anbesse et al. 2017; Asokan et al. 2012; Cajucom-Uy et al. 2010; Panchapakesan et al. 1998; Paula et al. 2006; Sherwin et al. 2011). Besides, it can also be detected via clinical diagnosis using a corneal topography machine to examine the presence of pterygium with topographic map visualisation (American Medical Association 2017; Minami et al. 2018; Ahmad et al. 2019). However, the current earlier screening and clinical diagnosis could be troublesome where it needs a well-trained ophthalmologist expertise within a specific procedure, and it takes time to carry out the diagnosis process. Since the transition towards technology, ophthalmologist experts have sought an automated approach for earlier pterygium detection and classification, which is less time-consuming. The widely used machine learning approach has developed rapidly in medical imaging. Digital image processing, also categorised as a machine learning method which involves hand-crafted heuristic methodology for feature extraction, has been implemented by previous researchers (Abbas 2017; Wang et al. 2018). Automated feature extraction has led to an advanced approach using DNN without hand-crafted feature extraction. DNN has been widely implemented in medical imaging and primarily focuses on eye diseases such as diabetic retinopathy using retinal images (Deepa et al. 2021) and optical coherence tomography images (Upadhyay et al. 2021). These automated approaches exist as an alternative to assist the expert in reducing diagnosis time. However, the implementation of DNN, which focuses on pterygium eye disease, is limited, and it requires large-scale datasets and high specifications appliances to obtain optimum performance. Therefore, patch region-based and data augmentation techniques are proposed in this experimental work. It acts as a data space solver (Lee & Chin 2020), besides developing a larger dataset scale compared to previous work (Zamani et al. 2020).

PREVIOUS WORK

There are very few published works on pterygium classification/detection using a deep learning approach, especially on deep neural networks. Previous work proposed a classification of ASPI between pterygium ASPI versus normal ASPI using a modified pretrained network (VggNet16-wbn) (Zamani et al. 2020). This project/literature has performed a few experimental works comparing existing classification networks. As a result, the best network, VggNet16, was modified with an additional batch normalisation layer and modification on the classification layer fixed with two ASPI classes. The modified network has surpassed all the experimented networks with 98.45% sensitivity, 99.22% accuracy and a perfect score for specificity and area under the curve performance. Both networks have been compared based on an activation map. Here, features of cornea circularity and the pterygium presence were highlighted to distinguish between pterygium ASPI and normal ASPI. The extracted features of pterygium can be highlighted with more visualisation by solely narrowing down to the pterygium ASPI database. However, the most critical part of DNN classification is the amount of data, whereby the pterygium ASPI database is half of the previous work data.

In the present work, we aim to ameliorate the presentation of extracted features through region-based with a limited amount of data using the previously proposed network architecture. The proposed experimental work is briefly explained in Section 3, followed by the presentation of experimental results with a discussion in Section 4. The summary of this work in Section 5 has concluded the experimental work with a suggestion for further research.

METHODOLOGY

In this section, a pterygium database and experimental work consisting of image pre-processing, data preparation in DNN, hyper-parameter setting, training and testing DNN, and analysis performance shall be briefly explained throughout the proposed method. A proposed block diagram is depicted in Figure 1. The proposed experimental work is accomplished using Matlab version 2018b with license no: 40699855 on NVIDIA GeForce RTX 2070 graphical processing units (GPU) desktop.

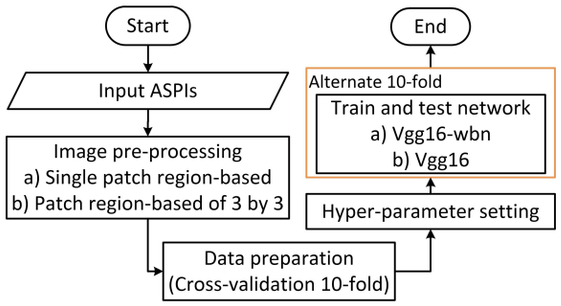

FIGURE 1. Proposed block diagram of pterygium classification using deep patch region-based ASPI

DATABASE DESCRIPTION

In this proposed method, two sets of experimental work are performed with two datasets, namely single patch region-based and patch region-based of 3 by 3. Both datasets are generated from pterygium ASPI for pterygium and nonpterygium cases. These datasets are acquired from a developed local database, namely myMata and have been used in previous work (Zamani et al. 2020) to classify pterygium and normal ASPI. A total of 30 pterygium ASPIs were captured using a high-resolution smartphone camera of Huawei P9 with co-engineered Leica. This database is developed in collaboration between the Faculty of Engineering and Built Environment and the Faculty of Health Science, both at Universiti Kebangsaan Malaysia, Malaysia. All the ASPIs are verified and validated by an ophthalmologist.

IMAGE PRE-PROCESSING

All the ASPIs for pterygium classification are processed and filtered based on pterygium tissue growth on either the nasal side or both sides of the eye ASPIs. A region with pterygium tissue is classified as a pterygium case, while a region with no pterygium tissue is classified as a nonpterygium case, as depicted in Figure 2. This pre-processing image method is called pterygia-patch.

SINGLE PATCH REGION-BASED ASPI

A single patch region-based ASPI database is generated by three steps of image pre-processing, as illustrated in Figure 2 a). Each sample ASPIs was divided vertically into three parts, and only the first and third horizontal regions of ASPIs are included in this patch region-based, as illustrated in Figure 2 a). The purpose of this division is to remove unwanted regions (region 2) not affected by pterygium tissue growth. Therefore, 60 images are produced, including 30 images of pterygium and 30 images of nonpterygium. Here, a single patch region-based dataset proceeded with image rescale before image augmentation was performed to increase the number of images. All the images were position augmented through process image reflection (both horizontally and vertically) and image rotation for every possible angle, which are 45 degrees, 90 degrees, 135 degrees, 225 degrees, 270 degrees and 315 degrees. A total of 240 images of pterygium and 240 images of nonpterygium were acquired and then underwent image enhancement to perform colour augmentation using the haze removal algorithm. This algorithm is commonly used for low-light images where dark and dim pixels are inverted to high contrast and enhance the image as illustrated in Figure 2 b) (colour augmentation). Hence, 1080 images were generated for a single patch region-based database.

PATCH REGION-BASED OF 3 BY 3 ASPI

The database of patch region-based of 3 by 3 is developed as a single patch region-based database development with the addition of patches step as illustrated in Figure 2 b). All images were patched into a small pixel of image size before it is fed into the training network. Before that, the images were rescaled to an image size of 255 x 255 from the original size to standardise the image for computational simplicity. Then, the image size of 255 was patched to the size of 85 x 85 images. This patching process produces nine patched images which need to be improved for efficient DNN classification with large-scale datasets. Hence, a commonly used technique to increase the number of datasets, namely data augmentation, was used. All image patches are augmented in position by reflection (horizontal and vertical). Therefore, the dataset consisted of 1080 patches of pterygium and nonpterygium, with 540 images each.

DATA PREPARATION (CROSS-VALIDATION)

Ten-fold cross-validation is conducted to ensure that the database can be generalised well and minimised the probability of underfitting and overfitting problems. These consequences could affect the performance of testing data and network training. This work divides all datasets into ten partitions (10% each). Therefore, one partition datasets consist of 108 images of a single patch and 108 image patches of 3 by 3, respectively. The ratio of data partition for both classes is randomly divided yet balanced to avoid imbalance data problems. Here, the network training would be performed on nine partitions and one partition for testing. Each partition is alternately tested 10-fold with 972 images used for network training and 108 testing images.

HYPER-PARAMETER SETTING

The deep neural network is generally performed using a network optimiser and several hyper-parameters to train the data, such as learning rate, batch size and the number of epochs. The network optimiser is crucial in assisting in optimising the network and minimising the loss function during network training. Thus, the mainly used optimisers are stochastic gradient descent with momentum (SGDM) and adaptive moment estimation (Adam) optimisers. These optimisers were tested to select which optimiser could converge faster. Adam computes adaptive learning rates individually (Kingma & Ba 2014). The network learns the features of data input by the rates of learning. The rate was tested with 0.1, 0.01, 0.001 and 0.0001 values. Besides, a hyper-parameter batch size of 32, 64 and 128 with a base power of 2 (2x) has been tested. These two hyper-parameters are tuned during network training with a few numbers of cycles. The learning cycles (epochs) determine the repetition of the learning process that depends on the quantity of training data sets called iteration. Here, the number of epochs was tested, starting with the lowest number, ten, to the highest possible number, such as 100. The performance was observed to determine which number of epochs accuracy stops improving, which then will be selected.

TRAINING AND TESTING NETWORK

The experimental work for datasets and networks that read the input images as a collection of matrices has been implemented. This work adopted a previously proposed network, namely VggNet16-wbn, a modified pretrained deep convolutional neural network of VggNet16 (Simonyan & Zisserman 2014) with 13 additional batch normalisation layers as illustrated in Figure 3.

All the input images were resized before entering the feature extraction layer to meet the input layer requirement of implemented networks. The input size networks are consistent with the same neuron number in the network input

layer. From the matrices, the training network performs the windowing process of the input image for feature extraction in the convolutional layer. The extracted features were mapped into specific sizes before being processed in the subsequent layers. The sensitivity of pixels in the feature map is then minimised as the batch normalisation layer has been implemented and followed by the activation layer, which is rectified linear unit (ReLU) to activate the feature map. These activated feature maps were resampled (pooling layer) and combined (fully connected layer) to calculate the probability of class percentage by softmax classifier.

PERFORMANCE ANALYSIS

The classification of the pterygium tissue using DNN is evaluated based on ground truth acquired in the myMata database from the optometry expert in the Faculty of Science and Health, UKM. Apart from training and testing both networks, the performance of the algorithm network is evaluated quantitatively through confusion metrics.

Generally, the confusion metrics are the quantitative evaluation to calculate the true positive (TP), false positive (FP), true negative (TN) and false negative (FN) between the binary classification. Here, performance metrics of experimental work are calculated to find the accuracy, sensitivity, specificity, and precision using (1-4), respectively.

$$accuracy = \frac{(\mathrm{TP}+\mathrm{TN})}{(TP+TN+FP+FN)} \quad (1)$$

$$sensitivity = \frac{\mathrm{TP}}{(TP+FN)} \quad (2)$$

$$specificity = \frac{\mathrm{TN}}{(TN+FP)} \quad (3)$$

$$precision = \frac{\mathrm{TP}}{(TP+FP)} \quad (4)$$

The quantitative performance of the network was supported by qualitative performance using gradient-weighted class activation mapping (GradCam) proposed by (Selvaraju et al. 2017). The interpretability technique of GradCam helps to visualise the active and important region of the image for the prediction of a network. GradCam function predicts the class score of the image by feature layer and reduction layer. The active region was selected by reducing the output to the image features in the feature layer.

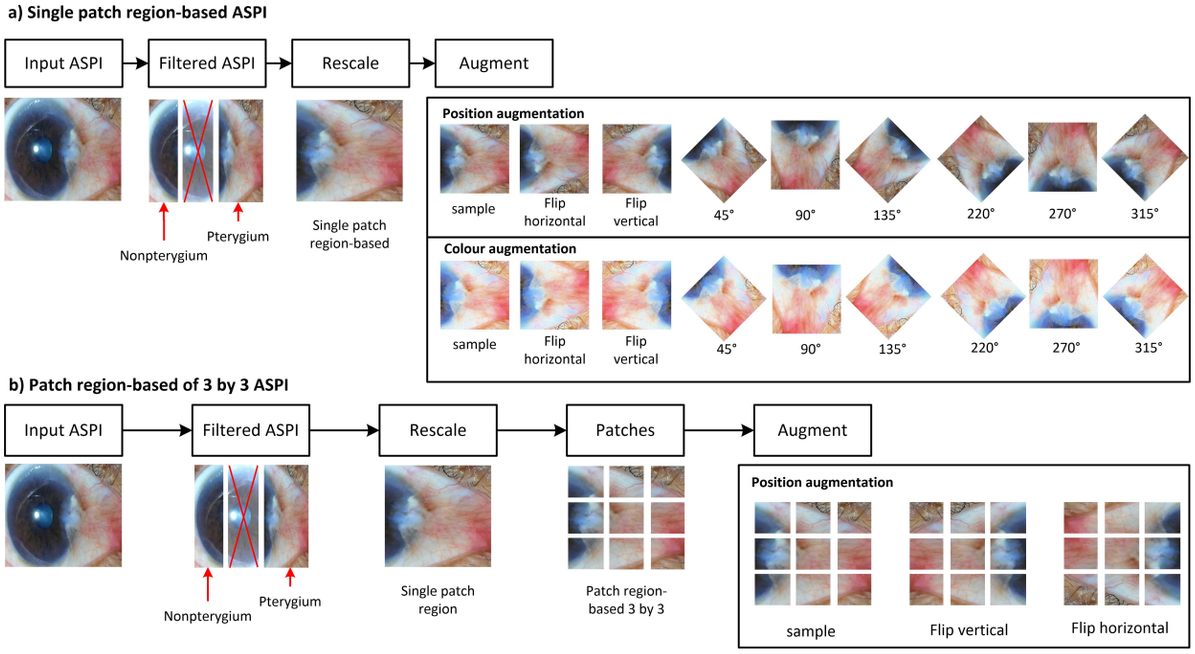

FIGURE 2. Pterygia-patch pre-processing method a) single patch region-based ASPI (top) with three steps of the pre-processing image which includes filter, rescale and augment, and b) patch region-based of 3 by 3 ASPI (bottom) with four image processing steps and addition of image patch

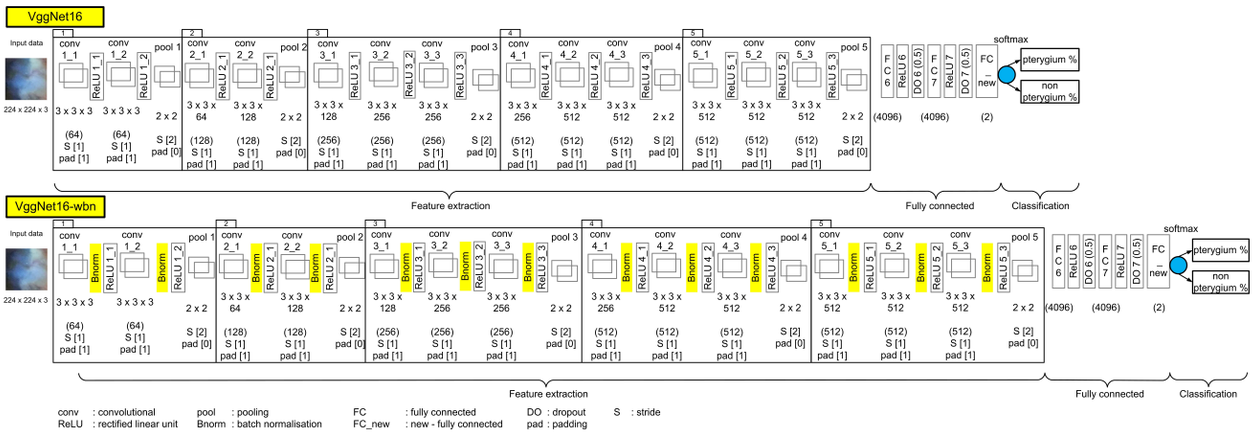

FIGURE 3. A deep patch-based pterygium tissue classification using the adopted proposed network architecture VggNet16-wbn (Zamani et al. 2020) and VggNet16 (Simonyan & Zisserman 2014)

RESULTS AND DISCUSSION

This experimental work evaluated the proposed method of classifying pterygium tissue using deep patch region-based on single and 3 by 3 image patches of ASPIs on VggNet16-wbn and VggNet16. These two experiments have performed 10-fold cross-validation using a fixed network optimiser and four values of hyper-parameters: Adam optimiser, 0.0001 learning rate, 64 size of batch and 74 epochs, respectively. These hyper-parameters values have been tested and analysed thoroughly; these were the most appropriate combination values. Adam optimiser has been chosen as the network converged well compared to the SGDM optimiser from the beginning until the end of the network training. Adam has adopted the first-order gradients with less memory since SGDM requires higher-order optimisation, which is unsuitable.

Furthermore, large-scale data requires high memory to perform the network training process. Hence, Adam was well suited for less memory requirement with a first-order gradient. The best performance recorded is a batch size of 64 compared to the poor performance of 32, and less complex and time-consuming than 128 during network training. The rate of 0.0001 is selected as the network finds and learns the input features well than others. Based on the combination hyper-parameters of a batch size of 64 and an optimum learning rate at 0.0001, network accuracy stops improving at 74 epochs.

In this work, four experimental works have been performed and evaluated by four performance metrics: accuracy, sensitivity, specificity, and precision, as listed in Table 1. Based on the quantitative performance in Table 1, a single patch region-based dataset, VggNet16-wbn achieved high performance than VggNet16 with 99.63% for all performance metrics. Both networks achieved the same sensitivity performance. Regardless, VggNet16-wbn has succeeded in increasing the probability of pterygium classification in accuracy and precision by 0.19% and 0.37%, respectively. The additional layer, batch normalisation, has succeeded in minimising the sensitivity of feature maps before the ReLU layer activates it. The sensitivity performance metric is significant for the network to classify true positives and false negatives of pterygium in avoiding misclassification of true class. This scenario is because misclassification could lead to misdiagnosis of true patients, which can hinder them from going through follow-up for further treatment. Misdiagnosis of a patient is the most unwanted incidence that can occur on the expert's behalf. Therefore, accuracy and sensitivity are crucial in medical imaging classification.

TABLE 1. A set of experimental work of two datasets using VggNet16-wbn and VggNet16

Dataset	Network	Accuracy	Sensitivity	Specificity	Precision
Single patch region-based	VggNet16-wbn	99.63	99.63	99.63	99.63
	VggNet16	99.44	99.63	99.26	99.26
Patch region-based of 3 by 3	VggNet16-wbn	95.19	96.67	93.70	93.88
	VggNet16	94.54	95.37	93.70	93.81

The image features in the patch region-based 3 by 3 datasets are more complicated as it contains unfixed features such as line and shape, unlike the single patch region-based dataset for the network, which is less complex. This feature representation has affected the patch region-based 3 by 3 classification performance, which achieved less than 99% of all performance metrics for both networks. However, VggNet16-wbn has achieved higher accuracy, sensitivity, and precision performance than VggNet16 with 95.19%, 96.67%, and 93.88%, respectively and the same specificity value of 93.70% with VggNet16. Figure 4 shows the confusion matrix for the single patch region-based to perceive a slight difference in the FP and TN prediction between the two networks.

The effectiveness of the networks was also evaluated in qualitative performance for robustness evaluation. The active region of the image can be visualised in GradCam, as illustrated in Figure 5. Based on qualitative observation, a single patch region-based dataset in Figure 5 a) depicts the VggNet16-wbn focusing on the nasal side as it is the common region of pterygium growth. The VggNet16-wbn detection covers pterygium tissue broadly, including the cornea encroachment, than VggNet16, where the network only focuses on the high visibility area of pterygium tissue. Pterygium tissue encroachment can be detected primarily on light green/yellow highlight and red highlight as the pterygium tissue thickens. On the other dataset, the detection area for patch region-based of 3 by 3, VggNet16-wbn is also able to detect most pterygium tissue area than VggNet16. However, in comparison for both datasets, the detected area for patch region-based 3 by 3 was not robust as it is scattered and could not find the exact pterygium pattern. Therefore, these observation shows VggNet16-wbn network has successfully detected the pterygium areas on the precise pterygium growth region using a single patch region-based.

In the meantime, the highlighted region on nonpterygium was affected by the quantitative performance of specificity. Figure 5 b) illustrates the region near perfectly covered, performed by VggNet16-wbn using a single patch region-based compared to the VggNet16 network. Here, the examined networks detect the highlighted region in the half-moon sclera as the nonpterygium focus area with no cornea encroachment. Meanwhile, the highlighted region using patch region-based of 3 by 3 looks mostly scattered as performed in pterygium. Therefore, the nonpterygium area could not be focused firmly. The focus area for both classes depended on quantitative performance. Whereby precision shows the exact highlighted area for pterygium growth (sensitivity) and nonpterygium (specificity). Hence, this qualitative performance has proven that the VggNet16-wbn network prediction is robust and effective on pterygium classification in terms of quantitative and qualitative performances.

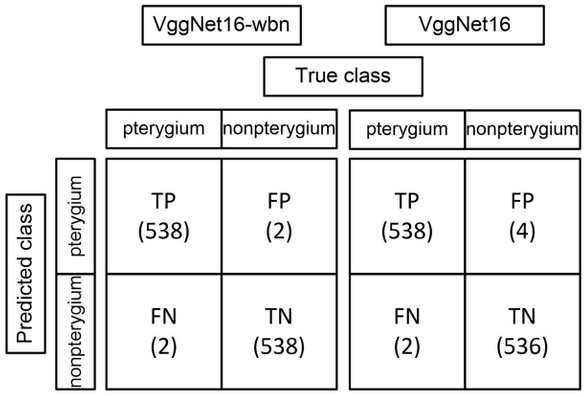

FIGURE 4. A confusion matrix for the single patch region-based

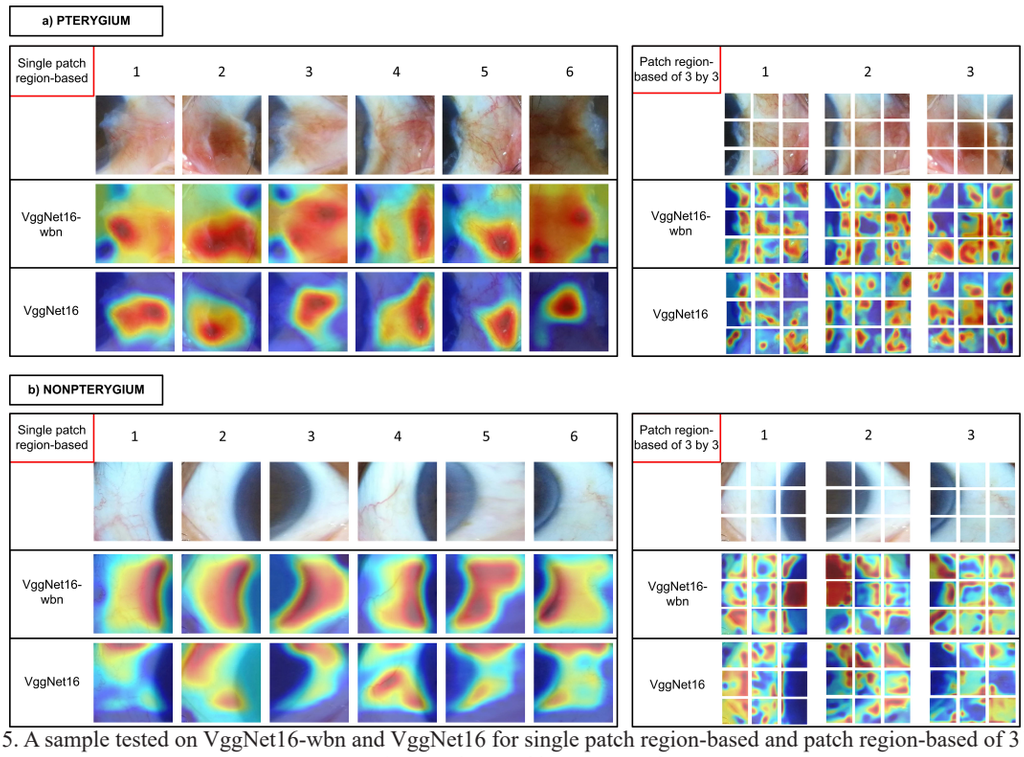

FIGURE 5. A sample tested on VggNet16-wbn and VggNet16 for single patch region-based and patch region-based of 3 by 3 datasets, a) pterygium and b) nonpterygium

CONCLUSION

Pterygium classification using deep patch region-based images developed from myMata ASPIs performs well in the adopted previous proposed network VggNet16-wbn and VggNet16. To our knowledge, no experimental work presents a patch region-based images approach in pterygium classification. Therefore, this is the first proposed experimental work of pterygium classification. A proposed patch region-based image is an alternative technique to solve the lack of data issues besides the data augmentation technique on pterygium ASPI. However, a large-scale dataset requires an appropriate combination of hyper-parameters and a small dataset to avoid overfitting and underfitting problems. In addition, accuracy and sensitivity performance metrics are the most important in the classification of medical imaging in minimising the chances of misclassification to avoid misdiagnosis of true class. The quantitative performance of a single patch region-based dataset using VggNet16-wbn outperforms VggNet16 with 99.63% accuracy, sensitivity, specificity, and precision on 10-fold cross-validation. The active region has been visualised through qualitative performance according to network prediction for both network and datasets using the GradCam technique. The VggNet16-wbn can focus on common pterygium growth regions with complete coverage of pterygium tissue, including cornea encroachment, as a robust and effective network prediction.

Moreover, the network is well generalised the data by implementing a cross-validation technique and minimises the chances of overfitting issues. In conclusion, a pterygium tissue classification using a deep patch region-based approach has been successfully accomplished. In future, the proposed experimental work of trained single patch region-based and patch region-based 3 by 3 datasets can be used as a baseline framework using limited datasets. In addition, the data collection of extracted pterygium features is vital for automated pterygium detection systems using artificial intelligence development.

ACKNOWLEDGEMENT

We wish to thank the Optometry and Vision Sciences Programme, School of Healthcare Sciences, Faculty of Health Sciences of Universiti Kebangsaan Malaysia for providing the facilities and resources for image data acquisition.

DECLARATION OF COMPETING INTEREST

None

REFERENCES

Abbas, Q. 2017. Glaucoma-deep: detection of glaucoma eye disease on retinal fundus images using deep learning. *International Journal of Advanced Computer Science and Applications* 8(6): 41–45. DOI:10.14569/IJACSA.2017.080606

Abdani, S. R., Zaki, W. M. D. W., Hussain, A. & Mustapha, A. 2015. An adaptive nonlinear enhancement method using sigmoid function for iris segmentation in pterygium cases. *International Electronics Symposium (IES). IEEE,* hlm. 53–57. DOI:10.1109/ELECSYM.2015.7380813

American Medical Association. 2017. *Medical policy: corneal topography*. Retrieved from http://jfs.ohio.gov/

Ahmad, S. N. A., Zaki, W. M. D. W. & Zamani, N. S. M. 2019. Sistem saringan penyakit pterigium untuk imej mata terangkum hadapan. *Jurnal Kejuruteraan* 31(1): 99-105. DOI: 10.17576/jkukm-2019-31(1)-12

Anbesse, D. H., Kassa, T., Kefyalew, B., Tasew, A., Atnie, A. & Desta, B. 2017. Prevalence and associated factors of pterygium among adults living in Gondar city, Northwest Ethiopia. *PLoS ONE* 12(3): 1–9. DOI:10.1371/journal.pone.0174450

Asokan, R., Venkatasubbu, R. S., Velumuri, L., Lingam, V. & George, R. 2012. Prevalence and associated factors for pterygium and pinguecula in a South Indian population. *Ophthalmic and Physiological Optics* 32(1): 39–44. DOI:10.1111/j.1475-1313.2011.00882.x

Bogdănici, C., Tone, S. & Bogdănici, T. 2013. Ocular changes in ophthalmo-heliosis. *Oftalmologia* 57(3): 9–18.

Cajucom-Uy, H., Tong, L., Wong, T. Y., Tay, W. T. & Saw, S. M. 2010. The prevalence of and risk factors for pterygium in an urban Malay population: the Singapore Malay Eye Study (SiMES). *British Journal of Ophthalmology* 94(8): 977–981. DOI:10.1136/bjo.2008.150847

Coroneo, M. 2011. Ultraviolet radiation and the anterior eye. *Eye and Contact Lens* 37(4): 214–224. DOI:10.1097/ICL.0b013e318223394e.

Coroneo, M. T., Müller-Stolzenburg, N. W. & Ho, A. 1991. Peripheral light focusing by the anterior eye and the ophthalmohelioses. *Ophthalmic Surgery, Lasers and Imaging Retina* 22(12): 705–711. DOI:10.3928/1542-8877-19911201-04.

Deepa, V., Kumar, C. S. & Cherian, T. 2021. Ensemble of multi-stage deep convolutional neural networks for automated grading of diabetic retinopathy using image patches. *Journal of King Saud University - Computer and Information Sciences* 1–11. DOI:10.1016/j.jksuci.2021.05.009.

Hill, J. C. 1989. Pathogenesis of pterygium. *Eye (Basingstoke)* 3(2): 218–226. DOI:10.1038/eye.1989.31.

Kingma, D. P. & Ba, J. L. 2014. Adam: a method for stochastic optimization. *arXiv preprint arXiv 1412.6980* 1–15. DOI:10.1063/1.4902458.

Kwok, L. S. & Coroneo, M. T. 1994. A model for pterygium formation. *Cornea* 13(3): 219–224. DOI:10.1097/00003226-199405000-00005.

Le, Q., Xiang, J., Cui, X., Zhou, X. & Xu, J. 2015. Prevalence and associated factors of pinguecula in a rural population in Shanghai, Eastern China. *Ophthalmic Epidemiology* 22(2): 130–138. DOI:10.3109/09286586.2015.1012269.

Lee, K. W. & Chin, R. K. Y. 2020. The effectiveness of data augmentation for melanoma skin cancer prediction using convolutional neural networks. *In 2020 IEEE 2nd International Conference on Artificial Intelligence in Engineering and Technology (IICAIET)*, hlm. 1–6. DOI:10.1109/IICAIET49801.2020.9257859.

Lucas, R. M., Mcmichael, A. J., Armstrong, B. K. & Smith, W. T. 2008. Estimating the global disease burden due to ultraviolet radiation exposure. *International Journal of Epidemiology* 37(3): 654–667. DOI:10.1093/ije/dyn017.

Minami, K., Miyata, K., Otani, A., Tokunaga, T., Tokuda, S. & Amano, S. 2018. Detection of increase in corneal irregularity due to pterygium using fourier series harmonic analyses with multiple diameters. *Japanese Journal of Ophthalmology* 62(3): 342–348. DOI:10.1007/s10384-018-0583-8.

Panchapakesan, J., Hourihan, F. & Mitchell, P. 1998. Prevalence of pterygium and pinguecula: The Blue Mountains Eye Study. *Australian and New Zealand Journal of Ophthalmology* 26: 52–55. DOI:10.1111/j.1442-9071.1998.tb01362.x.

Paula, J. S., Thorn, F. & Cruz, A. 2006. Prevalence of pterygium and cataract in indigenous populations of the Brazilian Amazon rain forest. *Eye* 20: 533–536. DOI:10.1038/sj.eye.6701917.

Selvaraju, R. R., Cogswell, M., Das, A., Vedantam, R., Parikh, D. & Batra, D. 2017. Grad-CAM: Visual explanations from deep networks via gradient-based localization. Proceedings of the IEEE International Conference on Computer Vision, hlm. 618–626. DOI:10.1109/ICCV.2017.74.

Sherwin, J. C., Hewitt, A. W., Kearns, L. S., Griffiths, L. R., MacKey, D. A. & Coroneo, M. T. 2011. The association between pterygium and conjunctival ultraviolet autofluorescence: The Norfolk Island Eye Study. *Acta Ophthalmologica* 91(4): 363–370. DOI:10.1111/j.1755-3768.2011.02314.x.

Simonyan, K. & Zisserman, A. 2014. Very deep convolutional networks for large-scale image recognition. *2014 International Conference on Learning Representations (ICLR),* hlm. 1–14. DOI:10.2146/ajhp170251.

Taylor, H. R. 1989. The biological effects of uv-b on the eye. *Photochemistry and Photobiology* 50(4): 489–492. DOI:10.1111/j.1751-1097.1989.tb05553.x.

Twelker, J. D., Bailey, I. L., Mannis, M. J. & Satariano, W. A. 2000. Evaluating pterygium severity: A survey of corneal specialists. *Cornea* 19(3): 292–296. DOI:10.1097/00003226-200005000-00007.

Upadhyay, P. K., Rastogi, S. & Kumar, K. V. 2021. Coherent convolution neural network based retinal disease detection using optical coherence tomographic images. *Journal of King Saud University - Computer and Information Sciences* 1–8. DOI:10.1016/j.jksuci.2021.12.002.

Vanicek, K., Frei, T., Litynska, Z. & Schmalwieser, A. 2000. UV-index for the public : a guide for publication and interpretation of solar UV index forecasts for the public. Retrieved from https://www.researchgate.net/publication/288523666_UV-Index_for_the_Public

Viso, E., Gude, F. & Rodrı´guez-Ares, M. 2011. Prevalence of pinguecula and pterygium in a general population in Spain. *Eye* 25(3): 350–357. DOI:10.1038/eye.2010.204.

Wang, J., Chen, Y., Hao, S., Peng, X. & Hu, L. 2018. Deep learning for sensor-based activity recognition: A Survey. *Pattern Recognition Letters* 1–10. DOI:10.1016/j.patrec.2018.02.010.

Yam, J. C. S. & Kwok, A. K. H. 2014. Ultraviolet light and ocular diseases. *International Ophthalmology* 34(2): 383–400. DOI:10.1007/s10792-013-9791-x.

Zamani, N. S. M., Zaki, W. M. D. W., Huddin, A. B., Hussain, A., Mutalib, H. A. & Ali, A. 2020. Automated pterygium detection using deep neural network. *IEEE Access* 8: 191659–191672. DOI:10.1109/access.2020.3030787.